Support Information

LiI doped MoS$_6$ composite for room temperature all-solid-state lithium batteries

Mingyuan Chang[a,c,d], Junjie Jia[a], Gaozhan Liu[a], Jianwen Zhang[c,d], Na Wang[a], Yangyang Zhou[a], Ping Cui[a,b], Tao Wu[c,d,e]*, Xiayin Yao[a,b]*

[a] Ningbo Institute of Materials Technology and Engineering, Chinese Academy of Sciences, Ningbo 315201, P.R. China

[b] Center of Materials Science and Optoelectronics Engineering, University of Chinese Academy of Sciences, Beijing 100049, P.R. China

[c] Municipal Key Laboratory of Clean Energy Technologies of Ningbo, University of Nottingham Ningbo China, Ningbo 315100, P.R. China

[d] Department of Chemical and Environmental Engineering, University of Nottingham Ningbo China, Ningbo 315100, P.R. China

[e] Key Laboratory of Carbonaceous Wastes Processing and Process Intensification of Zhejiang

* Corresponding authors: tao.wu@nottingham.edu.cn; yaoxy@nimte.ac.cn

Experimental section

Preparation of MoS$_6$ and 95MoS$_6$·5LiI

MoS$_6$ was prepared by wet chemical method. In a typically process, 0.2 g of iodine was dissolved in *N, N*-dimethylformamide; afterward, 0.28g of (NH$_4$)$_2$Mo$_2$S$_{12}$[S1] dissolved in *N, N*-dimethylformamide was added under stirring until a black precipitate formed. The as-prepared MoS$_6$ was filtered and washed with *N, N*-dimethylformamide, CS$_2$, and acetone, then dried in vacuum condition. For the 95MoS$_6$·5LiI (mol %) composite, a mixture of MoS$_6$ and LiI was mechanically milled with a planetary ball mill for 9 h at 510 rpm in argon atmosphere.

Characterization

The crystal structure of the samples was performed by X-ray diffractions (XRD, D8 Advance Davinci, Bruker). Time-of-flight secondary ion mass spectroscopy (TOF-SIMS, IONTOF TOF.SIMS 5) was employed to demonstrate the ionic bonds differentiation. The inductively coupled plasma emission spectrometer analysis (ICP-OES, Spectro Arcos, Spectro) was conducted to confirm the atom ratio. Field emission scanning electron microscopy (SEM, S-4800, Hitachi), scanning transmission electron microscopy-energy dispersive spectroscopy (STEM-EDS) and high-resolution transmission electron microscopy (HRTEM, FEI Tecnai F20) were employed to confirm the morphology, particle size and elements distribution of the samples.

Assembly and electrochemical performance testing of all-solid-state lithium batteries

The as-synthesized MoS$_6$ or 95MoS$_6$·5LiI composites were mixed with Li$_{10}$GeP$_2$S$_{12}$ and Super P in mass ratio of 40:50:10. Afterward, 150 mg of Li$_6$PS$_5$Cl solid electrolytes were cold pressed into pellets under 240 MPa. The ion conductivity of Li$_6$PS$_5$Cl sulfide solid electrolyte is 3.5×10^{-3} S cm^{-1}. Then, the above-mentioned composite cathodes were uniformly spread on the electrolyte surface and

cold pressed under 240 MPa. Finally, a piece of lithium foil was placed on the other side of the solid electrolyte pellet by pressing them together under 360 MPa. All the process were conducted in argon atmosphere.

The electrochemical impedance spectroscopy (EIS) and cyclic voltammetry (CV) tests were performed by the electrochemical work station (Solartron 1470E). The frequency range of EIS was set from 1.0 MHz to 0.1 Hz with the amplitude of 10 mV. The CV curves were conducted within the potential range of 1.0–3.0 V for all-solid-sate lithium batteries at different scanning rate. Charge/discharge profiles was collected on multi-channel battery test system (LAND CT-2001 A) under various current densities with voltage range of 1.0–3.0 V (vs Li/Li$^+$) at room temperature. The galvanostatic intermittent titration technique (GITT) was tested under 0.1 A g^{-1} for 5 min followed by rest for 120 min. The batteries were tested under the argon atmosphere.
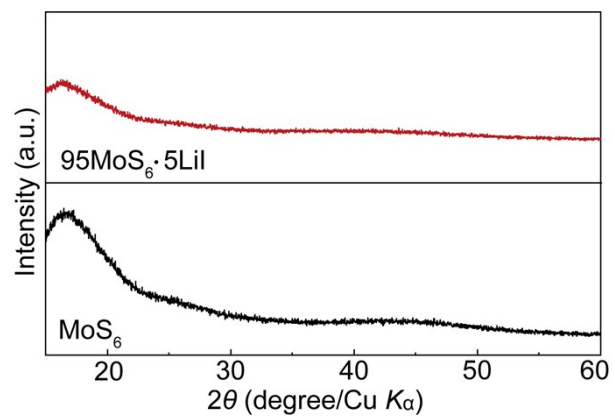
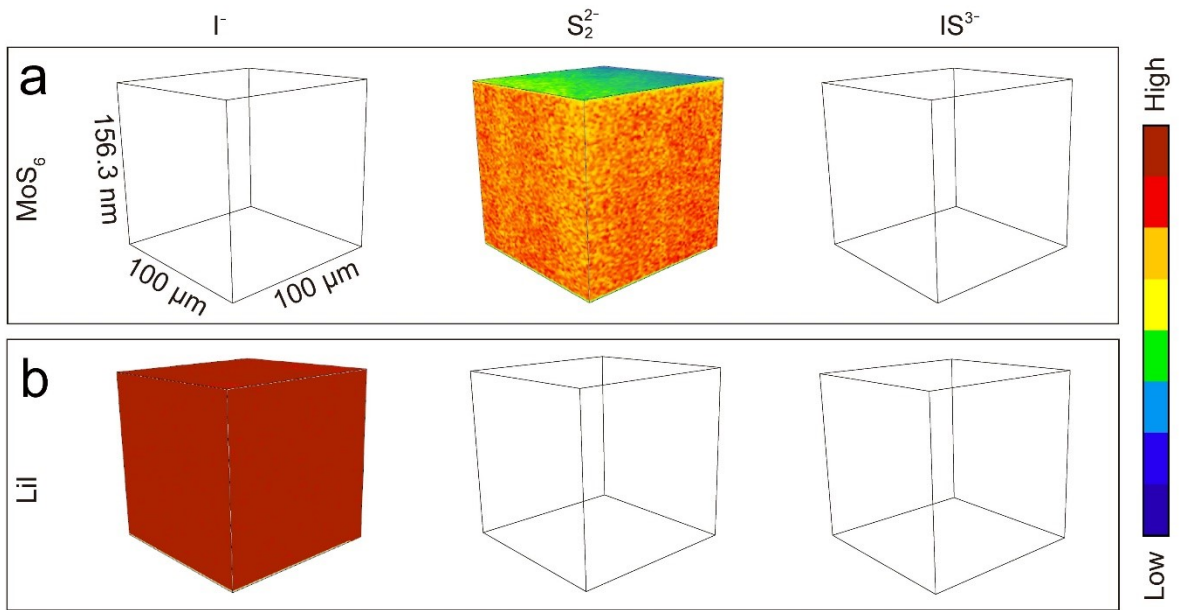Fig. S1 XRD patterns of MoS_6 and $95MoS_6 \cdot 5LiI$ composite

Fig S2. TOF-SIMS 3D distribution images of I$^-$, S_2^{2-} and IS^{3-} ions for (a) MoS$_6$ and (b) LiI.
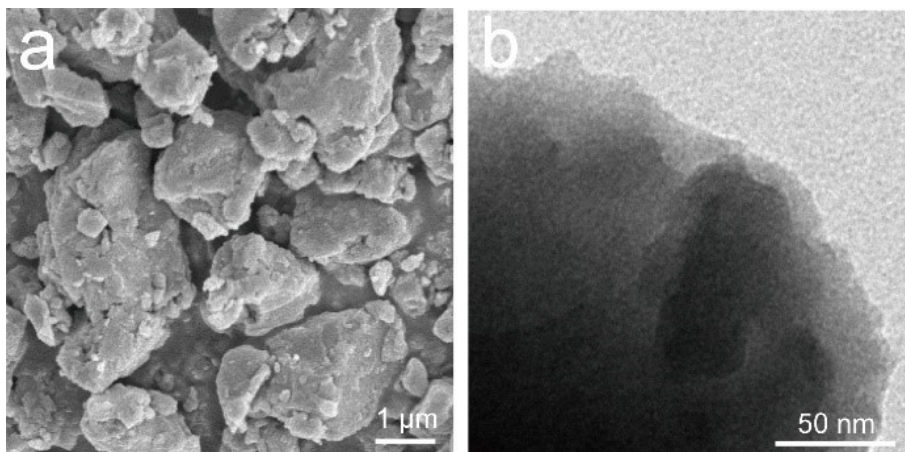
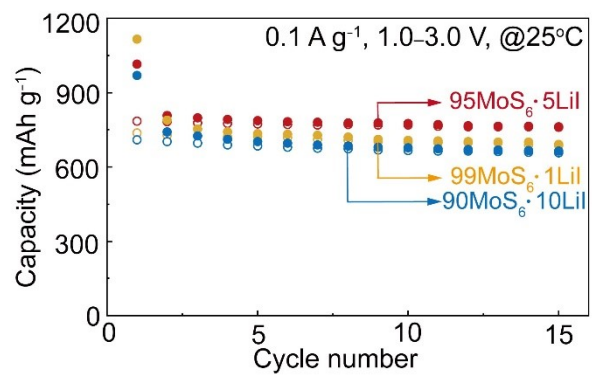Fig. S3 (a) SEM and (b) TEM images of MoS$_6$.

Fig. S4 Cyclic performances of 90MoS$_6$·10LiI, 99MoS$_6$·1LiI and 95MoS$_6$·5LiI composite under 0.1 A g^{-1}.
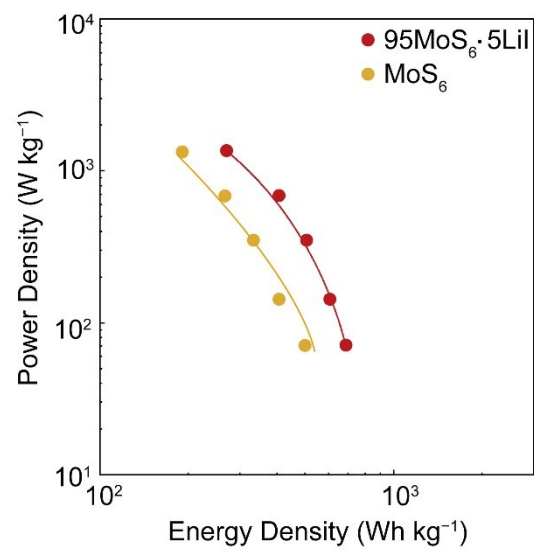
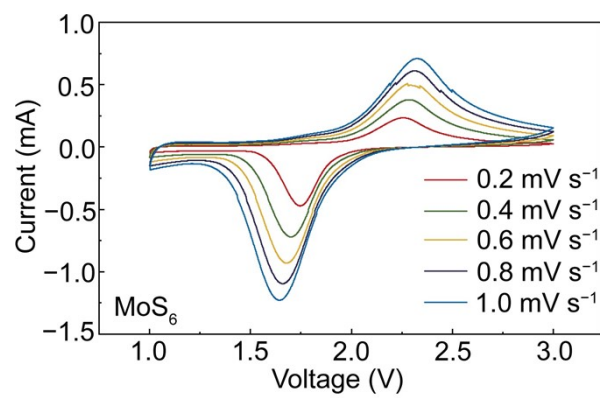Fig. S5 Ragone plots deduced from the rate performances in Figure 2f.
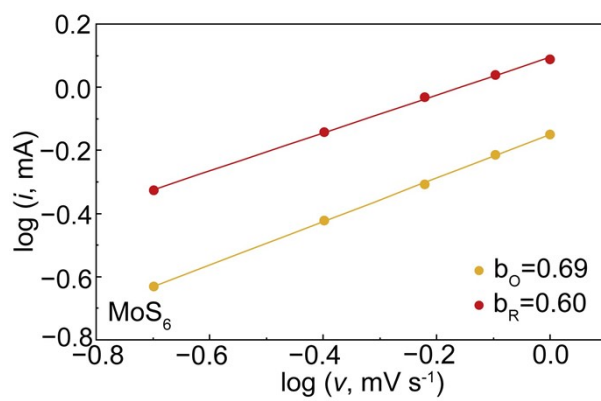
Fig. S6 CV curves of MoS_6 with various scan rates.

Fig. S7 The log (peak current) *vs.* log (scan rate) plots and fitted lines for reduction and oxidation peaks of MoS_6.
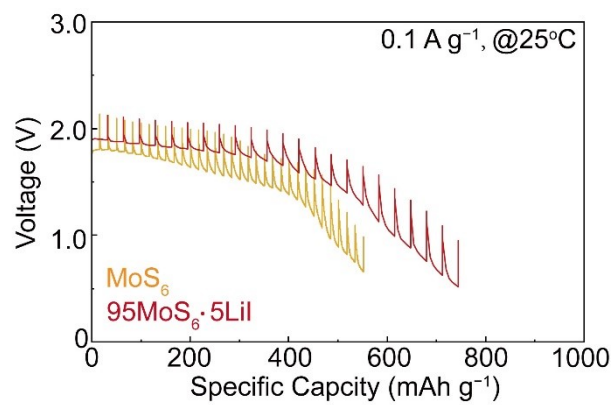
Fig. S8 GITT plot of Li/Li$_6$PS$_5$Cl/95MoS$_6$·5LiI and Li/Li$_6$PS$_5$Cl/MoS$_6$ all-solid-state lithium batteries.

Table. S1 EIS fitting results of MoS_6 and $95MoS_6 \cdot 5LiI$ composites under 1 A g^{-1} after 500 cycles.

Cathode material	1st cycle		500th cycle	
	R_e (Ω)	R_{ct} (Ω)	R_e (Ω)	R_{ct} (Ω)
MoS_6	69.87	/	605.71	447.82
$95MoS_6 \cdot 5LiI$	52.58	/	208.36	352.25

Reference

S1. M. Y. Chang, M. L. Yang, W. R. Xie, F. L. Tian, G. Z. Liu, P. Cui, T. Wu and X. Y. Yao, *Batteries-Basel*, 2023, **9**, 560.